Taylor & Francis
Taylor & Francis Group

Derivation and Integration of Shallow-Water Bathymetry: Implications for Coastal Terrain Modeling and Subsequent Analyses

KYLE R. HOGREFE,[1] DAWN J. WRIGHT,[1] AND
ERIC J. HOCHBERG[2]

[1]Department of Geosciences, Oregon State University, Corvallis, Oregon, USA
[2]Nova Southeastern University, Oceanographic Center, Dania Beach, Florida, USA

Satellite and acoustic remote sensing enable the collection of high-resolution seafloor bathymetry data for integration with terrestrial elevations into coastal terrain models. A model of Tutuila Island, American Samoa, is created using depths derived from IKONOS satellite imagery to provide data in the near-shore gap between sea level and the beginning of sonar data at 10–15 m depth. A derivation method gauging the relative attenuation of blue and green spectral radiation is proven the most effective of several proposed in recent literature. The resulting coastal terrain model is shown to be accurate through statistical analyses and topographic profiles.

Introduction

Coastal terrain models (CTMs) incorporating both topography and bathymetry, grounded by a geographic information system (GIS), have proven to be powerful analytical tools for the modeling of watershed and coastal morphology (Li et al. 2001; Jiang et al. 2004). The integration of environmental and societal data sets into a CTM enable investigations into the relationships and interactions of island ecosystems and provide information about terrestrial influences to coral reefs from human activities (Mumby et al. 2004). The marine and terrestrial components of island ecosystems are linked by fresh water inputs that reach miles out to sea and provide for nutrient exchange and larval transport, but they also carry sediment and pollutants that diminish the species diversity of coral reef community structure (Andrefouet et al. 2002; Shapiro and Rohmann 2005). Other research links diminished reef species diversity to human development density through the increased turbidity that it causes at the island scale (Sealey 2004). A finer scale investigation, at the watershed level, may reveal more direct relationships between land use practices, freshwater plumes and coral reef health.
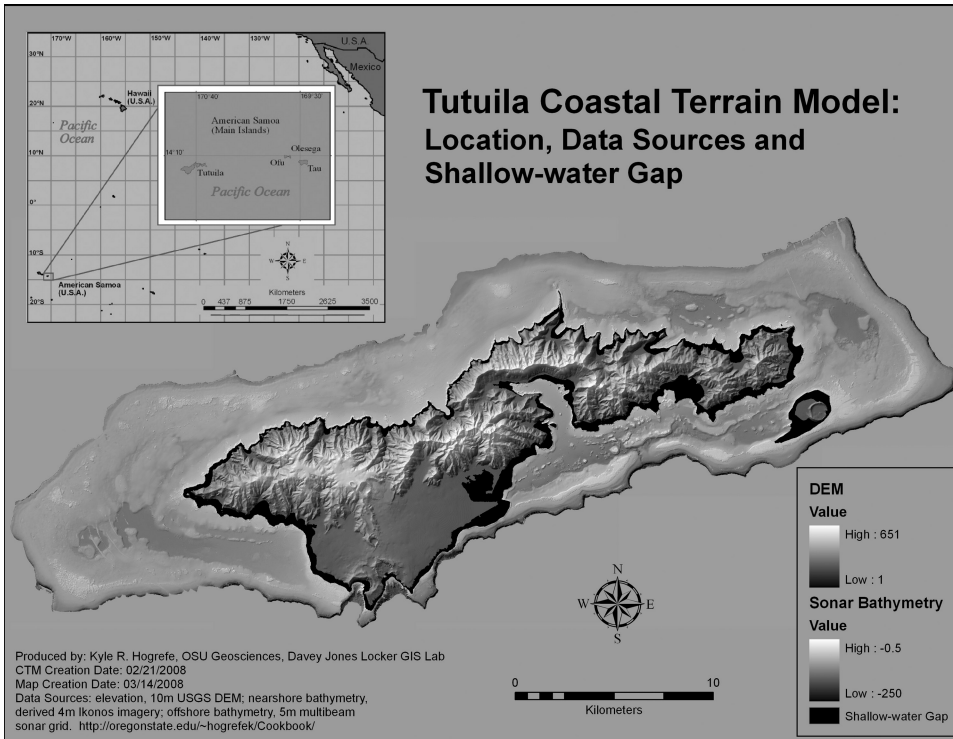
Figure 1. The island of Tutuila, American Samoa. Data sources include a 10-m USGS digital eleva-tion model (DEM) and offshore bathymetry at 5-m resolution, primarily from the NOAA Coral Reef Ecosystem Division (CRED) (more information online at oregonstate.edu/~hogrefek/Cookbook). Projection and datum are Universal Transverse Mercator (UTM) Zone 2 South, World Geodetic System (WGS) 1984. Notice the gap in data between the island and the deepwater bathymetry. Black regions show shallow-water data gaps.

Satellite and acoustic remote sensing technologies produce readily accessible data to create coastal terrain models detailed enough to run oceanographic, hydrographic, and atmospheric simulations (Mumby et al. 2004; Shapiro and Rohmann 2005). However, a particular challenge in the creation of a CTM is the acquisition of data from 0 to 15 m where surf conditions and shallow terrain features make the operation of bathymetric survey vessels hazardous (Figure 1). In clear water conditions, both LIDAR (light detection and ranging) surveys and processed satellite imagery show promise for filling this data gap. Though LIDAR data are more accurate, survey costs may be prohibitive while satellite imagery is more easily available and cost effective, particularly in remote locations or poor countries (Mumby et al. 1999). Recent work (Hochberg et al. 2007) investigates the accuracy of several methods proposed to derive bathymetry and points to one process (Lyzenga 1985) as the most effective. Similar methods, coupled with processing steps to eliminate surface glint, are used to derive bathymetry from IKONOS satellite imagery. These data are used in creation of a CTM for the island of Tutuila and its surrounding bathymetry and are subjected to error analysis during CTM integration.

Personal experience with community leaders, resource managers, and the general population on Tutuila as well as recent research (Wright 2002, 2004) indicate a strong

desire to take action to protect marine resources. However, the mitigation of pollutants in terrestrial runoff is problematic because it requires changing social practices, which further requires either extensive outreach and education or passage of regulations to modify people's actions. These solutions demand scientific information to convince individuals of the necessity of change or to justify the implementation of new policies (Hoffman 2002; Mumby et al. 1999).

Methods

Study Area

This research focuses on deriving bathymetry to complement pre-existing datasets for the creation of a CTM for the island of Tutuila, American Samoa (Figure 1), and testing its accuracy for the assessment of human population and land use practices on coral reefs. Tutuila is ideal for a case study of human driven terrestrial impacts. Its volcanic origin and the tropical climate of the South Seas have resulted in topography of well-defined ridgelines and valleys that extend beyond the shoreline to significant depth. These distinct marine/terrestrial units provide naturally defined topographic basins for comparing land use impacts to adjacent reefs. The population pattern of the island consists of valleys that contain human settlements ranging from cities such as Pago Pago (population ∼4,000) to small villages of populations of fewer than 100, with some small valleys remaining uninhabited. Though most of the settlement is concentrated on relatively flat coastal terrain, population pressure pushes development up steeper valley slopes and traditional land use, such as small plot agriculture and the harvest of fruit and wood, occurs farther up in the valleys. Pago Pago Harbor supports industrial activities such as a fish cannery and port services to support an extensive fishing fleet and international commerce. Densely populated areas spread along the coast southwest of Pago Pago Harbor and cross through several watersheds. These communities have many impervious surfaces that probably enhance runoff and contribute to pollutant loads.

Data

IKONOS imagery. The IKONOS satellite is a high spatial resolution "push broom" sensor with a sun synchronous polar orbit operated by GeoEye, Inc. The instrument obtains multi-spectral data in four bands at 4 m nominal resolution and panchromatic data at 1 m nominal resolution (Table 1). IKONOS images were originally obtained by NOAA Coastal Services center in 2001 and used to create a mosaic covering the islands of Tutuila and Aunu'u for the Pacific Islands GIS project. NOAA's National Centers for Coastal Ocean Science, Center for Coastal Monitoring and Assessment (CCMA) provide original imagery for this research. The images were acquired on 7 November 2001, 2 December 2001 (two images) and 3 February 2002 at approximately 21:44 hours and delivered as NTF files.

Multibeam sonar data. The Coral Reef Ecosystem Division (CRED) of NOAA's Pacific Islands Fisheries Science Center (PIFSC) in conjunction with the University of Hawaii's Pacific Islands Benthic Habitat Mapping Center provides bathymetry from 15–250 m depth. The data were collected from January to March 2004 and February to March 2006 using the 30 kHz Simrad EM300 and 300 kHz Simrad EM3002D sonar systems aboard the NOAA *R/V Hi'ialakai,* a 218-foot research ship. Also, a 240 kHz RESON 8101-ER sonar system

Table 1
IKONOS spatial and spectral resolutions

Band	Spectral range (μm)	Color range	Resolution (m at nadir)
1	0.45–0.52	Blue	4×4
2	0.52–0.60	Green	4×4
3	0.63–0.69	Red	4×4
4	0.76–0.90	Near-infrared	4×4
Pan	0.45–0.90	Panchromatic	1×1

was used aboard the *R/V AHI* (Acoustic Habitat Investigator), a 25′ survey launch operated by the PIFSC. The effort supports the Coral Reef Conservation Program goal of mapping all coral reefs in less than 30 m depth, and select reefs in deeper water, by 2009. Sonar soundings were processed into 5 m resolution raster grid and the data were provided as an ASCII file.

The projection and resolution of the deepwater bathymetry were chosen as project defaults so that, once the file was converted to an ESRI raster and defined in its projection, no further processing was required prior to CTM mosaicing. However, data gaps are apparent in the bathymetry in areas where sonar swaths did not overlap (Figure 1). An expression is employed using the ArcGrid command line window to close these data gaps using a moving average algorithm that assigns a mean value to "NoData" cell values without changing the original data.

Digital elevation model. The source of terrestrial data is a 10 m resolution mosaic of 1:24,000 scale USGS digital elevation models (DEMs) produced in April 2001 for the American Samoa Land Grant Extension program and provided to the American Samoa GIS User Group. Raster data grids derived from the original DEMs were mosaicked using ArcGIS to create the compilation. This product is the baseline dataset for terrain analysis on Tutuila and has previously been merged with bathymetric data around the island, but the shallow-water data gap prevents a seamless surface (Figure 1). To prepare the DEM for integration into the CTM, it is reprojected from the North American Datum of 1983, Geodetic Reference System (GRS) 1980 ellipsoid to World Geodetic System (WGS) 1984, Universal Transverse Mercator (UTM) 2S and resampled from a 10 m to a 5 m resolution.

Ground-truth data. Data points used to conduct error analysis on the derived bathymetry and the CTM are from two sources: recently collected control points and points created in ArcGIS with depth extracted from the PIBHMC multibeam sonar bathymetry. NOAA CRED's Oceanography Team collected most of the field survey control points during the 2008 American Samoa Research and Management Program research cruise. At each control point, position and depth data are collected either haphazardly or at specific waypoints. A small number of additional points are gleaned from oceanographic sampling records (CTD casts) from previous cruises. Each data point was collected using a Gramin76 GPS unit and an echosounder. The 140 resultant control points fall within all categories of bathymetric data used in the CTM. To more fully explore the range of error associated with the data, two additional sets of point features are used to extract sonar and derived depth values

for comparison. The first set entails the same point features used to extract the linearized spectral values used in determining the depth/spectral decay relationship (next section). Using these same points to evaluate derived depths may be considered biased; however, given that they were chosen in areas where image conditions looked most favorable for a clean spectral signal, they are useful for an analysis focused on areas likely to have a reasonable result. For an error analysis with greater geographic coverage and less bias, features of more than 800 points with haphazard distribution were created for each IKONOS image to extract derived values from depths shallower than 20 m as defined by the sonar bathymetry.

Bathymetric Derivations from IKONOS Satellite Imagery

Digital image processing techniques allow for the derivation of shallow water bathymetry by assessing the relative radiance of blue and green bands (Table 1) of the electromagnetic spectrum as they are attenuated as a function of depth. Bathymetric derivation procedures require starting with "at sensor" data, as provided by the CCMA, to assure accurate tracking of processing lineage and the validity of derived depth. The high spatial resolution of the IKONOS imagery makes the data suitable for detection of features with subtle relief and intricate structure (Stumpf et al. 2003; Mumby et al. 2004; Shapiro and Rohmann 2005). Depth derivation from spectral data is a multi-phase procedure using ArcGIS 9.2 (Environmental Systems Research Institute, Inc., Redlands, Calif.), ENVI 4.3 (ITT Industries, Inc., Boulder, Colo.), Microsoft Excel (Microsoft Corporation, Redmond, Wash.), and S-Plus (Insightful Corporation, Seattle, Wash.).

The four images required to cover the extent of Tutuila and Aunu'u were georectified and then converted from digital number to radiance values, using standard processing techniques. Sea surface glint effects were corrected using methods first described in (Hochberg et al. 2003) and refined by (Hedley et al. 2005) using the equation $R'_i = R_i - b_i(R_{NIR} - Min_{NIR})$; where R_i = radiance of band i, b_i = regression line slope of band i (y axis) against the NIR band (x axis), R_{NIR} = NIR radiance, and Min_{NIR} = minimum NIR value. The variable b_i is determined using a spatial subset of image pixels over optically deep water (>15 m) to obtain radiance values for the linear regression; Min_{NIR} may also be determined from this subset. The values R_i and R_{NIR} are drawn from the input image as it is processed. However, Tutuila CTM bathymetric derivations employ a modified version of this formula by not subtracting the Min_{NIR} value to correct for atmosphere in the same manner as a "dark pixel subtraction." Therefore, corrections for both sea surface glint and atmospheric effects are conducted using the formula $R'_i = R_i - b_i(R_{NIR})$. The linear regression between band i radiance and NIR radiance is calculated using MS Excel, while ENVI 4.3 enables other processing steps.

In recent work, a variety of bathymetric derivation procedures proposed since 1978 are tested using imagery from various sites across the Pacific (Hochberg et al. 2007). Figure 2 shows the results of an error analysis of the four most effective methods compared with SHOALS (Scanning Hydrographic Operational Airborne LIDAR Survey) data in Kaneohe Bay, Oahu, Hawaii. One method (Lyzenga 1985) far outperforms the others achieving an error range of +5 m to −5 m, that is half the size of the others. Note that the 5 m overestimate occurs at a depth of 5 m while the 5 m underestimate occurs at a depth of 20 m. Similar results are obtained when methods based on Lyzenga (1985) are used to derive shallow water bathymetry for inclusion in the Tutuila CTM.

Bathymetric data are derived by gauging the relative attenuation rates of blue (450–520 nm) and green (520–600 nm) spectral radiation as it passes through the water column.
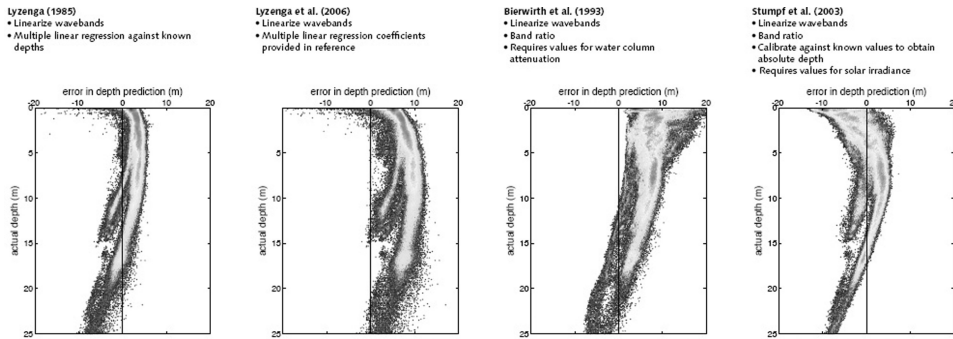
Figure 2. Error analyses for four published methods to derive bathymetry, all from high-resolution QuickBird satellite imagery. Derived depths from an image of Kaneohe Bay, Hawaii are compared to SHOALS (Scanning Hydrographic Operational Airborne LIDAR Survey) data. The y-axis represents increasing depth while the x-axis shows the negative and positive error of the derived depth.

Spectral values are first linearized using the formula $R_{Linear} = Ln(R_i - R_{imin})$; where R_i = radiance of band i, and R_{imin} = minimum radiance of band i. The variable R_i is drawn from the input image as it is processed while R_{imin} is determined using a spatial subset over optically deep water from the glint/atmosphere corrected image. With this step completed in ENVI 4.3, the linearized spectral data for the blue and green bands are exported to ArcGIS 9.2 for data extraction, a process greatly facilitated by the ENVI Reader for ArcGIS plug-in (http://www.ittvis.com/), to establish correlation with depth in a multiple linear regression using S-PLUS.

In ArcMap, features containing between 150 and 200 points are created for each IKONOS image extent in depths of less than 20 m and then used to extract sonar depth and linearized blue and green spectral values at each location. The multiple linear regression analysis is conducted with depth as the dependant variable and the linearized spectral values as the independent variables. The outputs of interest are y-intercept, and the slope for each spectral band. Depth is then derived in ENVI 4.3 using the equation $D = a + (b_i)(x_i) + (b_j)(x_j)$; where a = y-intercept, b = slope, x = linearized spectral value and i and j indicate spectral band. The variables x_i and x_j are drawn from the input image as it is processed. The four ENVI raster files containing derived bathymetry are then opened in ArcGIS, converted to ESRI grid files and mosaicked into a single raster grid. The derived bathymetry mosaic is then resampled to a resolution of 5 m and erroneous values from cells over optically deep water are trimmed in preparation for final integration into the CTM.

Data Set Integration

The CTM mosaic provides terrain data from the 650 m peak of the island to 250 m depth using the IKONOS derived bathymetry to fill the critical shallow water gap of 0–15 m. The integration of the CTM is accomplished using ArcGIS 9.2. Original datasets for the CTM are standardized to the geographic reference of the WGS84, UTM Zone 2 South.

The integration sequence entails merging the derived data from each image into a mosaic, combining the multibeam and derived bathymetry grids, and adding the DEM data. During the mosaic process data priority is first given to derived values from images that perform best in the error analysis described below, then to the sonar values so that they replace derived values in areas of overlap and finally to the DEM. After the derived/sonar

data integration, a gap fill expression is then applied through a sequence of 46 iterations to completely fill all "NoData" values. Most of the smaller gaps including, between swath widths, from terrain shadows and in surf zones, are filled after four iterations of the expression, but large voids remain from extensive areas of cloud cover. The last 42 iterations are required to provide information in these areas and result in far more dubious values; this issue is explored further below. The expression also adds values around the perimeter and into the center of the combined bathymetry grids, which are resolved by trimming the perimeter and by the DEM prioritization, described above.

Results

The accuracy of both the derived bathymetry and integrated CTM data are assessed at multiple stages of data processing and integration using depth control points collected during field surveys and points features created to extract sonar depth data as controls. The ability of the derived data to detect terrain features, as well as the utility of the integrated CTM for providing seamless terrain across datasets, are evaluated using linear transects that cross both natural features and transition zones between the data sources.

Derived Bathymetry Error Analysis

Control points from both field surveys and sonar data extraction are used for linear regression analyses plotting the control depth (x) against the derived depth (y) to compare the accuracy of derivations from each image (Figure 3). The image specific data sets are then combined to extract values from the derived imagery mosaic after resampling (Figure 4). The four images needed to cover the extent of Tutuila are referred to as West Tutuila, West-central Tutuila, East-central Tutuila, and East Tutuila, and they are presented in this geographic order across the columns of Figure 3. The indicators of quality and error in these graphs are the slope of the linear fit to the data and the r^2 value. The plotted control depths represent a "correct" linear relationship with a slope of 1. The further the value of the regression line's slope is from 0 toward 1, the greater the sensitivity to spectral signal attenuation with depth in the derived bathymetry values. Of course, the higher the r^2 value the more consistently close the derived values are to the control values.

Looking to the focused sample data, for example, it is clear that the derived bathymetry from West-central image is the best product with a slope of 0.238 and an r^2 value of 0.238, followed by the East-central with a slope of 0.136 and an r^2 value of 0.110, East with a slope of 0.140 and an r^2 value of 0.073, and West Tutuila with a slope of 0.103 and an r^2 value of 0.034. Though the magnitude of these measures varies between the focused, haphazard and control point error analyses, this pattern of data quality is consistent between images. The fact that the most favorable results are exhibited by the control point data set, the most direct link to reality, has positive implications for the use of these data for terrain modeling. In a more immediate sense this information guided the prioritizing of image values during the mosaic process so that the best results were retained. However, the second best image, East-central Tutuila, had such extensive data loss due to cloud cover that it made sense to prioritize the data from the third best image, East Tutuila, in the derived bathymetry data mosaic. The only data available for the western portion of the island was that with the most tenuous results.

The progression of derived depth quality across the images is explained by variable atmospheric and sea-state conditions at the time of data acquisition of each of the four images. The images were acquired on three dates over the course of three months and exhibit
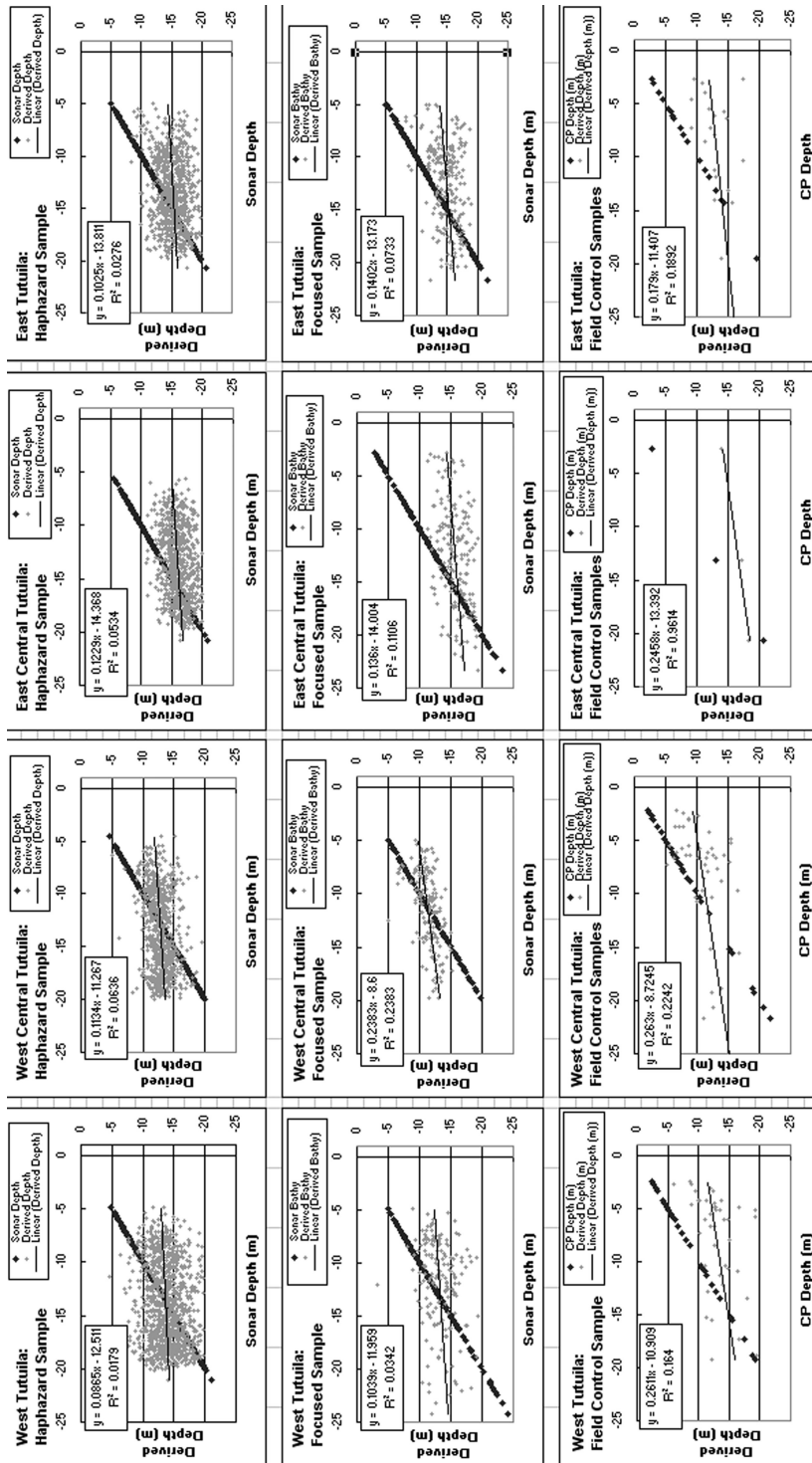
Figure 3. Derived bathymetry error analysis by linear regression. Notice that each column represents a satellite image and each row represents a point sample type.
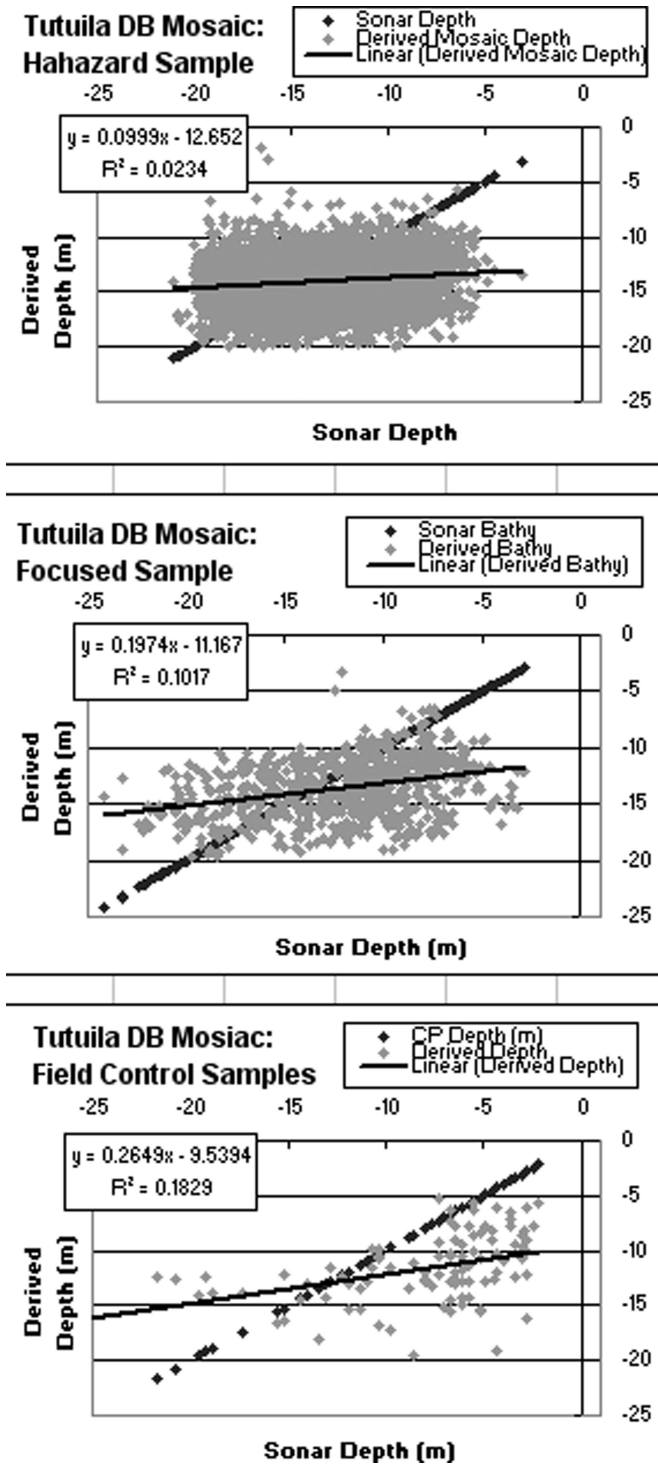
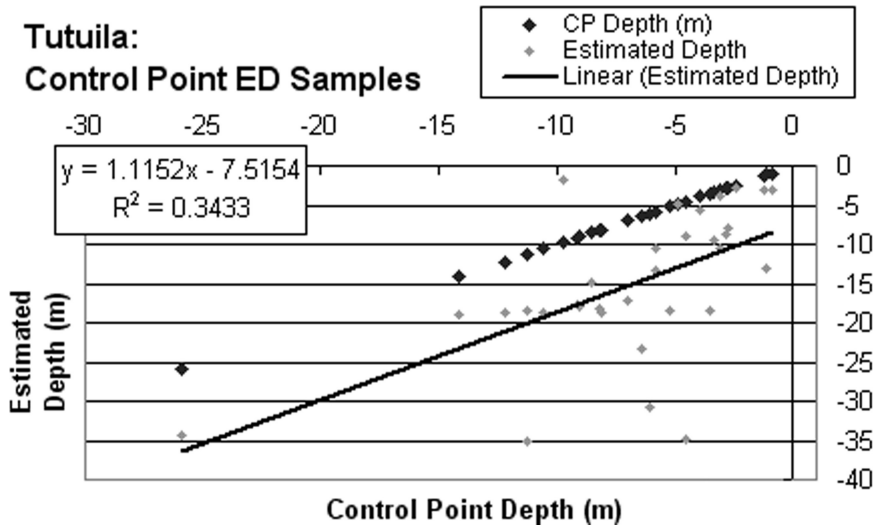**Figure 4.** Error analysis by linear regression performed on integrated derived bathymetry.

a range of ocean swell, wind wave (chop), and sea spray conditions. More wave action causes a greater range of sea-glint values and frothy waves within a pixel's ground coverage area create erroneous spectral signals that result in less accurate sea glint corrections. Wind-blown sea spray, a particular problem in near shore areas close to breaking waves, increases the non-selective scattering of spectral energy and therefore increases the error in atmospheric correction for the effected pixels. These errors compound through processing and result in less accurate depth derivations as exemplified by the results in Figure 3, where the best results correlate with the best environmental conditions in the original imagery.

The prioritization of datasets during mosaic integration and interpolations during the resampling of the mosaic grid from a 4 m to a 5 m resolution result in new values at many locations in the derived bathymetry mosaic. Therefore, the point features are aggregated and used to extract values from the mosaic for a final quality assessment previous to integration into the greater CTM (Figure 4). The same pattern of increasing slope and r^2 values through the haphazard, focused and control point data sets apparent in the image specific analysis is also obvious in the mosaic data error analysis. Though this trend may be attributable to decreasing sample size, it has positive implications for the inclusion of the derived bathymetry in the CTM. The haphazard sample clearly shows the potential error in the derived bathymetry in the depth of the data cloud, but even this "broadest net" sample of derived values shows a weak correlation. The statistical results improved markedly using the data points from the focused sample, but these data are suspect for error analysis since the same points were used to extract the linearized spectral values used in the depth derivation process. Herein lays the particular value of the CRED control point data, which were collected in a haphazard manner as the Oceanography Team completed other deployment duties around Tutuila. Where positions were provided to guide their efforts, they were chosen only on the presumption of shallow depths in the area and the only guiding criteria was that control point depths be less than 15 m. The control point slope value of 0.264 and r^2 value of 0.182 demonstrate a high degree of correlation between on site depth measurements and derived depth values using unbiased sample locations.

CTM Error Analysis

With the derived bathymetry integrated into the full CTM mosaic, the CRED control points serve for two final error analyses. Of the original 140 control points, 103 fell within areas of derived bathymetry and have been used in the previous analysis (41 in West Tutuila, 47 in West-central Tutuila, 3 in East-central Tutuila, and 21 in East Tutuila—with overlap), 32 fell within areas of estimate depth, and 5 fell in areas covered by multibeam sonar. The points within areas of estimated depth are used to assess the values calculated by the ArcGrid moving mean expression in areas void of data, while the full set of 140 points is used to extract values from the CTM for a final analysis of the fully integrated mosaic. Because of this control point spread, the final CTM error analysis can be considered inclusive of all data types with a focus on the derived bathymetry.

Cloud cover in the original IKONOS imagery necessitates that a significant area of the near shore bathymetry is estimated using the mean value of surrounding cells. Multiple iterations of the algorithm are needed to fill the larger gaps with the estimated surface error increasing with distance from the edge of "real data." Figure 5 demonstrates the utility and relative accuracy of the estimated depths with a slope of 1.115 that is actually steeper than that of the control data and a high r^2 of 0.343, however, the large potential error in the data is illustrated by the outliers in the range of 30–35 m of estimated depth and 5–12 m control depth.

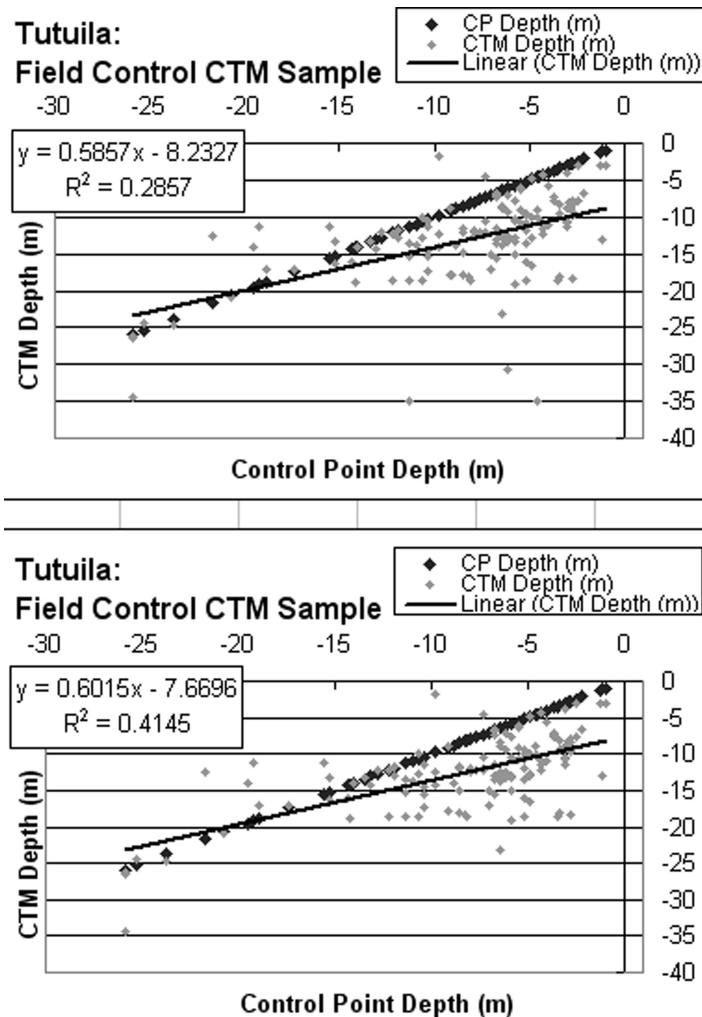**Figure 5.** Error analysis by linear regression performed on estimated bathymetry.

With the derived and estimated bathymetry thus validated, and the DEM and multibeam sonar datasets presumed to be accurate on their own merits, a final error assessment of the integrated CTM is conducted using the 140 CRED control points to extract depth data from the CTM. Regression analyses of these data results in an initial slope of 0.585 and r^2 value of 0.285 which improve to a slope of 0.601 and r^2 value of 0.414 with the removal of 3 outliers (Figure 6) signifying a statistically valid representation.

These final figures conclude the extended error analysis of multiple stages of bathymetric derivation and CTM integration and provide support for the use of bathymetry derived from IKONOS imagery to provide shallow water depth data for coastal terrain modeling. Though the model is not perfect, analyses show that the derived depths represent a realistic measure of depth and that overall error decreased as the datasets are mosaicked into the CTM. Further analyses provide evidence that the derived data's range of error is small enough to provide realistic terrain through the sea-land transition and justifies additional steps to smooth seems between the data sets.

Data Set Seams and Morphological Detail

In addition to the error analyses, linear transects are created to extract elevation and depth data across the land-sea interface to visualize and quantify the vertical offset at the seams between the DEM, derived bathymetry, and multibeam sonar data sets. The transect profiles are also used to explore the CTM's representation of subtle topographic transitions and detection of specific terrain features. Four transects are created as point features in ArcGIS with a value extracted from each contiguous raster cell over distances of 800 m or 1200 m (Figure 7). The extracted data result in terrain profiles with a 5 m horizontal spacing and vertical reliefs of 50 m, 80 m, or 200 m over transitions between the DEM, derived bathymetry (DB), ArcGrid expression estimated bathymetry (EB), and sonar bathymetry (SB) data (Figures 8–11).

Transect 1 (Figure 8) begins on the floodplain of a small watershed and follows the hollow of the basin into an offshore submarine channel. The "stepping" on the left side

Figure 6. Error analysis by linear regression performed on complete CTM mosaic.

of the profile is an artifact inherent on low slopes in data originating as an integer DEM. A vertical offset of 6.7 m is readily apparent at the transition between the DEM and EB. However, no offset exists at the transitions from EB to DB (at a distance of 510 m), which is as should be expected since the ArcGrid expression derived the EB values as the mean of nearby DB values. There is also no offset from DB to SB (at a distance of 720 m), which simply shows excellent corroboration between the two sources of depth data.

Transect 2 (Figure 9) starts at the top of a ridge, descends quickly before crossing a narrow reef flat, proceeds across a channel with two small ridges and then crosses a large coral plateau. At the land-sea transition, the first DB value has a drastic vertical offset of 19.2 m, but subsequent DB values are much more realistic and provide for good terrain representation across the reef flat to a seam without vertical offset between DB and SB at a distance of 215 m. From this point to a distance of 435 m ridges in the bottom of the channel are clearly indicated by SB data. There are two transitions from SB to DB and back
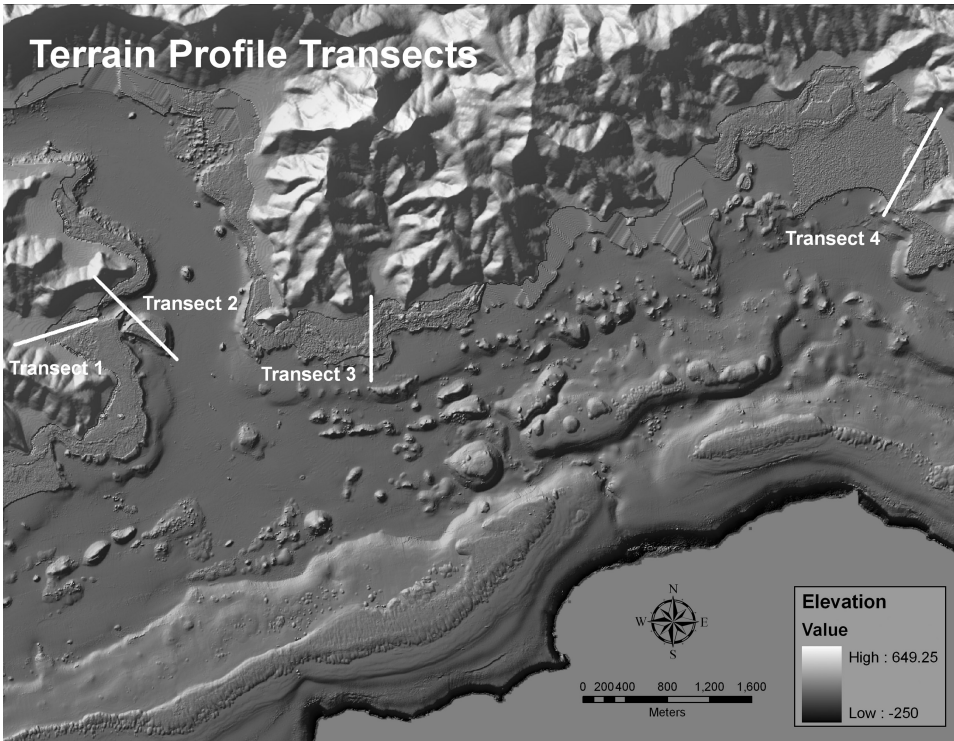
Figure 7. Tutuila CTM with terrain profile transects.

at 440 m and 665 m with vertical offsets of only 2.5 m and 2.3 m as the transect crosses the coral plateau.

Transect 3 (Figure 10) initiates at the base of a ridge crossing a steep grade to the shoreline, proceeds across a broad back reef and reef crest before ending on the fore reef slope. There is a vertical offset of 5.67 m between the DEM and the DB at the land-sea interface. From this transition to a distance of 400 m, the profile exhibits typical back reef terrain with moderate rugosity and variable depth that increases until a sudden decrease at the reef flat, which causes a notable data issue. At a distance of 330 m the DB values began to thin out (in the derived bathymetry mosaic) due to surf conditions and breaking waves on the reef flat, and the depth values become "more estimated" to the right. The other side of this surf zone data gap is at a distance of 675 m in the SB data where the depth values become "more estimated" to the left on the profile. The drastic vertical offset
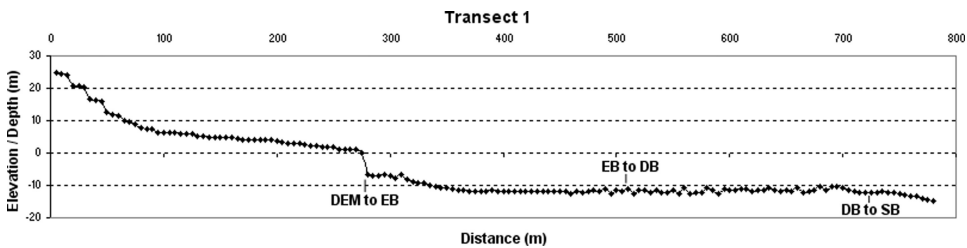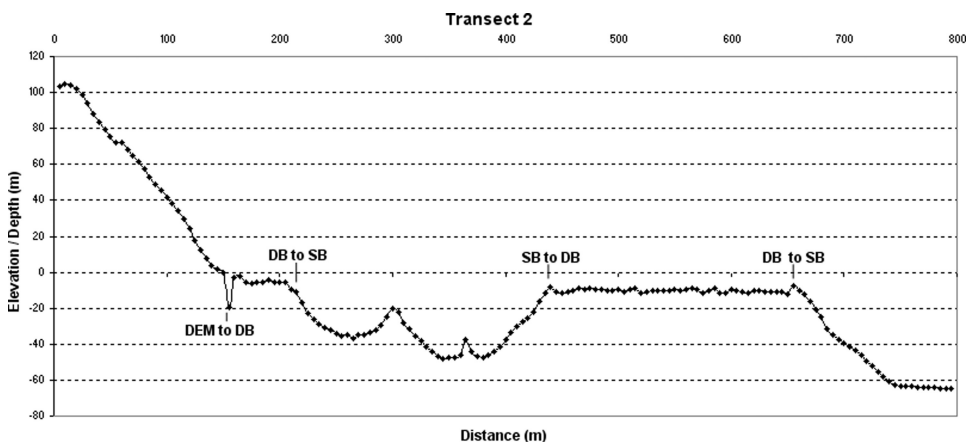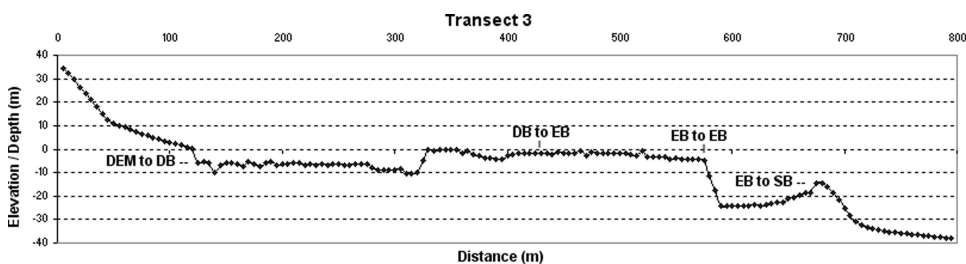

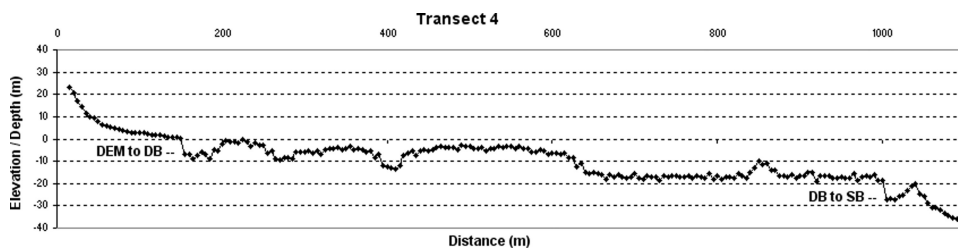**Figure 8.** Terrain profile of Transect 1.

Figure 9. Terrain profile of Transect 2.

of 19.5 m between distances of 575 m and 590 m is the transition between EB calculated from original DB and SB data during several iterations of the ArcGrid expression run to fill the data gap. The large error at this seam is a result of the EB data failing to capture the real change in depth from the shallows at the edge of the DB values to the deeper reef slope SB values.

Transect 4 (Figure 11) runs from the base of a ridge across a moderately sloped coastal plain to the shoreline, proceeds across a narrow back reef and then continues along the fore reef while crossing a channel and then finally descends the reef slope. There is a vertical offset of 6.74 m between the DEM and the DB at the land-sea interface. From this point to a distance of 640 m the DB profile again indicates typical back reef / fore reef morphology and closer inspection of the terrain that transect 4 crosses reveals that the DB data provide a high degree of detail allowing for the detection of potholes in the variable terrain of the shallows and the channel in the fore-reef at a distance of about 400 m. One of the limitations of the bathymetric derivation method is evident between the distances of 665 m and 1000 m. The derived depth data bottoms out at the lower range of the derivation procedure's effective limit of around 15 m (in this case) until the transect crosses the tip of a fore reef outcrop that is in range from of 835 m to 875 m distance. The vertical offset of 9.1 m at distance of 1005 m is the transition between this "false floor" artifact and the SB data. This data artifact is also apparent in Figure 7, in the middle of the bay to the west of transect 4, where most of the data in the central bay are false floor with a vertical offset of up to 35 m at the seam. Fortunately for the model, this is the only area around the island with such a

Figure 10. Terrain profile of Transect 3.

Figure 11. Terrain profile of Transect 4.

large gap between the effective range of the derived bathymetry and the extent of the sonar bathymetry data set.

This generation of the Tutuila CTM was integrated with the intent of leaving the artifacts and errors that are inherent in the original data or that result from derived bathymetry processing and CTM integration so they might be scrutinized. The error analyses presented in this section demonstrate that, though the data are not perfect, the derived bathymetry is reasonably correlated to control data and effective at detecting subtle terrain features, thus supporting its integration into the final CTM mosaic. It is further demonstrated by the terrain transect profiles that the combined topo/bathymetric product, though the transition between data sets are not always seamless, is an accurate enough representation of reality to justify its continued refinement and further use in terrain analysis research.

Discussion

Improvement and Repeatability of Derivation Method

The current iteration of Tutuila CTM provides a foundation for efforts to smooth extreme values at the seams of data sets and explore options to provide better data in areas where clouds, surf, or depths beyond the detection floor create a data gap should also be explored. Metadata for the sonar bathymetry indicate that the raw sonar data were cleaned of erroneous "noise" values and then smoothed with a high pass filter previous to conversion to a raster grid. These preprocessing steps remove extreme values and improve the modeled terrain surface and, therefore, should be conducted with the derived bathymetry mosaic, particularly the high pass filter. Further, when the derived depth grid is mosaicked with the sonar bathymetry, the edges of the data sets should be "feathered," a commonly available processing option, to create a transition zone of averaged values from both data sets to reduce the vertical offset at the seams.

Step-by-step documentation of processing methods and suggestions concerning the nuances of using ENVI, ArcGIS, Excel, and S-Plus to derive bathymetry and create the CTM are provided in a processing "cookbook" that should enable similar products at other locations (Hogrefe 2008a). However, the cookbook does not represent a formal set of instructions as several of the steps require familiarity with GIScience concepts and technology along with the judgment of experience when the "recipe" needs to be adjusted. Creation of a model using the guidance of the cookbook would support the validity of this research and meet a goal of this study in creating repeatable method for the creation of coastal zone models.

Issues with Merging Data Sets

Data gaps. The issues of whether and how to fill areas of "NoData" values in the derived and sonar bathymetry grids remain to be considered. As the IKONOS data are processed, areas of cloud cover and breaking surf are masked out of the imagery as unsuitable spectral data for depth estimation. As the multibeam sonar data are collected, data gaps result in strips where sonar swaths do not overlap and behind sharp terrain features that cause "signal shadow." Regardless of the cause, these data gaps raise the question of whether they should be left in the data or filled using data interpolation methods. It may be argued that filling these areas with estimated values results in a product of dubious validity because the data are not from the direct sensing of depth in that area. However, a continuous surface should prove superior for terrain and current modeling, so the goal for this research is the creation and testing of such a surface.

To this end, an ArcGrid command line expression is used to apply a moving average algorithm that assigns the mean value from a 6×6 window to "NoData" cells without changing original data values. The estimated surface could be further improved by using control points and other data to "seed" the large data gaps with depth measurements to provide accurate input for the ArcGrid algorithm as it calculates depth. This measure will not only create more site-specific precision but will also result in less extreme vertical offsets for the feathering function to address at data set seams. Of course, new satellite imagery without clouds in the same locations would be the best solution for filling the cloud gaps, but this analysis seeks solutions with the given materials.

Vertical datum issue. A matter concerning the accurate integration of bathymetric and topographic data sets remains in the form of the vertical datum issue. Having assured two of three primary components of a common geospatial framework with the same coordinate system and horizontal datum, the more intractable problem of converting to a common vertical datum is circumvented but not actually resolved. Vertical datum specifications may be tidal, based on regional tidal measurement, orthographic, derived from gravity potential, or geodetic, created using space based systems. Bathymetric data are usually referenced to a tidal datum such as mean lower low water (MLLW), which is the case for the multibeam data, while topographic data are usually based off an orthographic datum such as the National Geodetic Vertical Datum of 1929 (NGVD29), which is the specific case with the Tutuila DEM. The Tampa Bay (Florida) Topobathy Project has developed tools that provide for conversions between 28 commonly used vertical datum specifications using a numerical hydrodynamic circulation models and spatial interpolations of tide level between gauge stations. The conversion to a common vertical datum avoids data conflicts at the sea/land interface, however, to date this tool is only available for limited regions of the continental United States and not available for American Samoa (Gesch and Wilson 2001).

While seeking a permanent solution for the conversion of the Tutuila data to a common vertical datum, the CTM integration is allowed to progress due to the nature of the data sets. The DEM and the deepwater bathymetric data do not overlap so that there is no specific data conflict at the sea-land interface, a common problem associated with the vertical datum issue. The error introduced by the vertical datum issue is also manageable. Though not applicable to Tutuila, the datum conversion tool indicates a vertical offset between NGVD29 and MLLW at Tampa Bay (28°N latitude) of only 0.326 m. Given that Tutuila (14°S latitude) is about half as far from the equator, with less tidal flux, it may be presumed that the vertical offset at this position would be even less. In addition, the island's steep

topography allows for little horizontal displacement of shoreline position even at a real tidal flux in the 1 m range. It is also relevant to note that the derived bathymetry is not vertically referenced at all, though a tide correction for the specific time the image was recorded might be considered. However, the error at the shallow and deep end of derivation method's range is greater than either this potential tidal correction of 0–.5 m or that of the vertical datum offset.

To solve the problem of establishing sea-level, which would still need to be addressed with the grids converted to the same vertical datum since neither data set actually crosses the sea-land interface, a ring of raster cells is added to the DEM with a value of 0.000001. This is accomplished by adding a ring of new raster values one to three cells thick around the DEM perimeter, reclassifying the entire new raster to the value 0.000001 (chosen since the value zero is involved several processing steps and can be problematic), and mosaicking it back to the original DEM. The result is a ring of sea level values that separate land and sea once the adjusted DEM is mosaicked to the previously integrated derived and sonar bathymetry grid.

Future Work

When a freshwater plume enters the ocean from its watershed, dispersal is affected by seafloor bathymetric interactions with shallow and deep currents determining the distribution of the plume's payload across the reef. Pathogens, nutrient loading, and high turbidity in the plumes are presumed to have a detrimental effect on reef health. The negative effects of these factors can be measured as a function of the diversity and distribution of coral, algae, invertebrate, and reef fish species (Salas et al. 2006; Mumby 2001). Differences in human settlement, population density, and land use patterns may lead to variable stream sediment load, nitrification, or pathogen levels in Tutuila's watersheds and have a corresponding effect on the species composition and diversity of coral and fish populations of adjacent reefs.

Topographically defined units over the sea-land interface should enable analyses of material and energy exchange that will help to identify the impact of terrestrial inputs to near shore marine environments. In terrestrial studies, hydrologic units are defined through the assessment of slope, aspect, and ridgeline location and enable the analysis of groundwater and surface runoff as a function of variable rainfall levels (Clarke and Burnett 2003; Miller et al. 2007). The expansion of this concept using the CTM to define island terrain in terms of marine-terrestrial units (MTU) that span the land-sea interface should enable quantitative scientific information correlating land use and development practices to the vitality of reef communities as measured by coral and fish species composition and diversity. This effort will contribute to an island-scale comparison conducted in the Caribbean (Sealey 2004), which found a correlation between population density and decreased reef species diversity, by refining its geographic focus. Such scientifically-valid information may enable American Samoa managers and community leaders to make informed decisions regarding the stewardship of Tutuila's terrestrial and marine resources (as exemplified in Hoffmann 2002; White et al. 2006).

Ongoing applications enabled by the classification of Tutuila's terrain into MTUs include advanced investigations into the dispersal of inputs from specific watersheds into their affiliated marine catchments and allow for comparisons among MTUs (Hogrefe 2008b). The greater CTM could then enable the analysis of topographic effects on terrestrial freshwater flows as well as surface and deep-sea currents to model the systemic dispersal of terrestrial plume loads.

Conclusion

Coral reefs are in decline across the globe and scientific literature increasingly points to anthropogenic factors, many of them with terrestrial origins, as primary drivers behind the degradation. Coastal terrain models that enable the modeling of material and energy exchange across the land-sea interface are effective analytical tools to study the interconnectivity of terrestrial and marine systems. Multiple publications since 1978 establish the efficacy of deriving bathymetry from spectral data. This work and the new analyses of the Tutuila CTM product prove that such data provide an accurate representation of reality. Though steps to improve the CTM during mosaic compilation are proposed, the current CTM is deemed of sufficient quality to be used in terrain studies employing the concept of marine/terrestrial units. Marine/terrestrial units will be used to compare human development and the vitality of coral reefs within the same topographical regions. Correlations would indicate that terrain restrains material flows between the land and sea while defining the impact of terrestrial inputs to the system. Specific results may be used to determine the impact of differing land use practices and population levels on adjacent coral reefs. This scientifically defensible information could then enable informed decision making by local community leaders and resource managers.

Acknowledgements

References

Andrefouet, S., P. J. Mumby, M. McField, C. Hu, and F. E. Muller-Karger. 2002. Revisiting coral reef connectivity. *Coral Reefs* 21(1):43–48.

Clarke, S. and K. Burnett. 2003. Comparison of digital elevation models for aquatic data development. *Photogrammetric Engineering and Remote Sensing* 69:1367–1375.

Gesch, D. and R. Wilson. 2001. Development of a seamless multisource topographic/bathymetric elevation model for Tampa Bay. *Marine Technology Society Journal* 35:58–64. Retrieved July 27, 2008, from http://chartmaker.ncd.noaa.gov/bathytopo

Hedley, J. D., A. R. Harborne, and P. J. Mumby. 2005. Simple and robust removal of sun glint for mapping shallow-water benthos. *International Journal of Remote Sensing* 26(10):2107–2112.

Hochberg, E. J., S. Andrefouet, and M. R. Tyler. 2003. Sea surface correction of high spatial resolution IKONOS images to improve bottom mapping in near-shore environments. *IEEE Transactions on Geoscience and Remote Sensing* 41(7):1724–1729.

Hochberg, E. J., S. Vogt, J. E. Miller and K. R. Hogrefe. 2007. Remote sensing of shallow water bathymetry for integration with multibeam SONAR data. *Pacific Region Integrated Data Enterprise principle investigators conference*, Honolulu, HI, Poster. Retrieved July 27, 2008, from http://apdrc.soest.hawaii.edu/PRIDE/pride_meetings.html

Hoffmann, T. C. 2002. The reimplementation of the Ra'ui: Coral reef management in Rarotonga, Cook Islands. *Coastal Management* 30(4):401–418.

Hogrefe, K. R. 2008a. Digital image processing "cookbook:" A method to derive bathymetric data from high spatial resolution multispectral imagery. Corvallis, OR:Davey Jones Locker Marine GIS Lab, Oregon State University. Retrieved July 27, 2008, from http://oregonstate.edu/~hogrefek/Cookbook/

Hogrefe, K. R. 2008b. Derivation of near-shore bathymetry from multispectral satellite imagery used in a coastal terrain model for the topographic analysis of human influence on coral reefs. M.S. Thesis, Corvallis, Oregon, Oregon State University.

Jiang, Y. W., O. W. H. Wai, H. S. Hong, and Y. S. Li. 2004. A geographical information system for marine management and its application to Xiamen Bay, China. *Journal of Coastal Research* 254–264.

Li R., J. Liu, and Y. Felus. 2001. Spatial modeling and analysis for shoreline change detection and coastal erosion monitoring. *Marine Geodesy* 24:1–12.

Lyzenga, D. R. 1985. Shallow-water bathymetry using combined LIDAR and passive multispectral scanner data. *International Journal of Remote Sensing* 6(1):115–125.

Miller S. N., D. J. Semmens, D. C. Goodrich, M. Hernandez, R. C. Miller, W. G. Kepner, and D. P. Guertin. 2007. The automated geospatial watershed assessment tool. *Environmental Modeling and Software* 22:365–377.

Mumby, P. J. 2001. Beta and habitat diversity in marine systems: A new approach to measurement, scaling and interpretation. *Oceologia* 128(2):274–280.

Mumby, P. J., E. P. Green, A. J. Edwards, and C. D. Clark. 1999. The cost-effectiveness of remote sensing for tropical coastal resources assessment and management. *Journal of Environmental Management* 55(3):157–166.

Mumby, P. J., W. Skirving, A. E. Strong, J. T. Hardy, E. F. LeDrew, E. J. Hochberg, R. P. Stumpf, and L. T. David. 2004. Remote sensing of coral reefs and their physical environment. *Marine Pollution Bulletin* 48(3–4):219–228.

Salas F., C. Marcos, J. M. Neto, J. Patricio, A. Perez-Ruzafa, and J. C. Marques. 2006. User-friendly guide for using benthic ecological indicators in coastal and marine quality assessment. *Ocean and Coastal Management* 49:308–331.

Sealey, K. S. 2004. Large-scale ecological impacts of development on tropical islands systems: comparison of developed and undeveloped islands in the central Bahamas. *Bulletin of Marine Science* 75(2):295–320.

Shapiro, A. C., and S. O. Rohmann. 2005. Summit-to-sea mapping and change detection using satellite imagery: tools for conservation and management of coral reefs. *Revista De Biologia Tropical* 53:185–193.

Stumpf, R. P., K. Holderied, and M. Sinclair. 2003. Determination of water depth with high-resolution satellite imagery over variable bottom types. *Limnology and Oceanography* 48(1):547–556.

White, A., E. Deguit, W. Jatulan, and L. Eisma-Osorio. 2006. Integrated coastal management in Philippine local governance: Evolution and benefits. *Coastal Management* 34(3):287–302.

Wright, D. 2002. Mapping and GIS capacity building in American Samoa. *Proceedings of the 22nd Annual ESRI User Conference*. San Diego, CA, Paper 101.

Wright, D. J. 2004. Marine geography in support of "reefs at risk." In *World minds: Geographical perspectives on 100 problems*, B. Warf, D. Janelle, and K. Hansen (eds.), pp. 325–330. New York: Kluwer Academic Publishers.